

論文 / 著書情報
Article / Book Information

論題(和文)	
Title	Top-Gathering Periodic Array Derived from the Self-Organization of Inorganic -Organic Hybrid Pillars
著者(和文)	瀬川浩代, 山崎康夫, 矢野哲司, 柴田 修一
Authors	Hiroyo Segawa, Yasuo Yamazaki, Tetsuji Yano, S. Shibata
出典 / Citation	J. Ceram.Soc. Jpn, Vol. 114, No. , pp. 120-124
Citation(English)	J. Ceram.Soc. Jpn, Vol. 114, No. , pp. 120-124
発行日 / Pub. date	2006,

Top-Gathering Periodic Array Derived from Self-Organization of Hybrid Organic–Inorganic Pillars

Hiroyo SEGAWA,^{*,**} Yasuo YAMAZAKI,^{*} Tetsuji YANO^{*} and Shuichi SHIBATA^{*}

^{*}Tokyo Institute of Technology, 2–12–1, O-okayama, Meguro-ku, Tokyo 152–8550

^{**}PRESTO-JST, Japan Science and Technology Corporation (JST), 4–1–8, Honcho, Kawaguchi-shi, Saitama 332–0012

有機–無機ハイブリッド材料の自己組織化による倒れ周期構造体の形成

瀬川浩代^{*,**} · 山崎康夫^{*} · 矢野哲司^{*} · 柴田修一^{*}

^{*}東京工業大学大学院理工学研究科, 152–8550 東京都目黒区大岡山 2–12–1

^{**}科学技術振興機構, 332–0012 埼玉県川口市本町 4–1–8

The mechanism of “top-gathering” pillars and the controllability of top-gathering pattern formation were investigated. Two-dimensional pillar arrays with micrometer repetitions have been fabricated from a hybrid organic–inorganic material by photolithography. The type of array structure formed depending on the distance between neighboring pillars. From in situ observation during drying, it was found that capillary force is affected by the distance between the pillars. Such pillars of 16 μm height were gathering, and top-gathering units could be obtained when the distance between neighboring pillars is less than 8 μm . Gathering units composed of four pillars can be formed periodically by controlling the arrangement of the pillars.

[Received September 15, 2005; Accepted October 20, 2005]

Key-words: Hybrid organic–inorganic material, Self-organization, Sol–gel, Capillary force

1. Introduction

Two-dimensional (2D) periodic arrays of dielectric materials with submicrometer to micrometer repetitions have been used in various devices such as photonic crystals and microlens arrays.^{1)–3)} These arrays are fabricated by conventional lithography using X-rays, electron beams, lasers or UV light. In lithography, a resist is initially coated on substrates of a dielectric material, and the resist is exposed to a light source such as an electron beam or a laser through a mask. After that, the resist is developed and rinsed in an appropriate solvent, then resist patterns are formed. The dielectric material is etched chemically in an area not covered with resist patterns. Finally, 2D periodic arrays are obtained. In the drying of the rinse solvent, resist patterns become unstable, and finally collapse or are distorted as aspect ratio (i.e., the ratio pillar height to pitch) increases.⁴⁾ Such pattern collapse is caused by the surface tension of the rinse solvent.^{4)–6)}

On the other hand, capillary force due to the surface tension of the rinse solvent is useful in making new patterns of photosensitive materials. Recently, 2D patterns of polyimide pillars have been fabricated by electron-beam lithography, and bunching structures of such pillars could be produced when the diameter of the pillar is very small.⁷⁾ We also reported “top-gathering” pillar arrays of a hybrid organic–inorganic material formed by self-organization.⁸⁾ Such pillars with micrometer repetitions are fabricated by UV light lithography and those with submicrometer repetitions by the laser interference technique,⁹⁾ in which laser beams split by a diffractive beam splitter are interfered and irradiated onto photosensitive films. When capillary force is controlled by array structure parameters such as pillar height, diameter and pitch, several pillars self-organize and gather at the top, and top-gathering pillar arrays are obtained. The top-gathering pillar arrays are particularly attractive for use as template in fabricating new structures such as pyramidal structures for electron luminescence components or photonic devices such as tunable photon-

ic crystals. However, it is difficult to control the number of pillars in a top-gathering unit and the period of the arrangement of top-gathering units, because the mechanism of top-gathering has not yet been clarified.

In our previous studies, hybrid organic–inorganic materials composed of inorganic networks modified with photosensitive organic molecules such as unsaturated hydrocarbon were used to fabricate 2D periodic arrays.^{8),10),11)} In photosensitive hybrid materials, we cannot only fabricate patterns easily without using a resist but also obtain inorganic patterns by the calcination and removal of organic components from the initial patterns of hybrid materials.^{12),13)} Top-gathering arrays of hybrid organic–inorganic materials are useful in the fabrication of complex inorganic patterns, which cannot be obtained by conventional lithography.

In this study, we fabricate various 2D pillar arrays with several micrometer repetitions by photolithography to clarify the origin of top-gathering and to control the top-gathering pattern formation of hybrid organic–inorganic pillars.

2. Experimental

A hybrid organic–inorganic material, which is suitable for the fabrication of periodic arrays by photolithography,⁸⁾ was prepared as a photosensitive film on a glass substrate by the sol–gel method. The material was fabricated from methacryloxypropyl trimethoxysilane (MAPTMS) and methacrylic acid (MA), both of which had photopolymerizable C=C double bond groups, and zirconium *n*-propoxide ($\text{Zr}(\text{OPr})_4$) as an inorganic network former. The molar ratio of MAPTMS to $\text{Zr}(\text{OPr})_4$ was 8 : 2. MAPTMS was hydrolyzed by adding HCl (pH = 2) and the mixture was stirred for 30 min. In another bottle, $\text{Zr}(\text{OPr})_4$ was chelated by adding MA and an equal volume of 1-PrOH, and the sol was stirred for 30 min. $\text{Zr}(\text{OPr})_4$ sol was added dropwise to the stirred MAPTMS sol and the mixture was stirred for 30 min. Then, water was added dropwise to the sol. IRGACURE184 (Chiba Specialty Chemi-

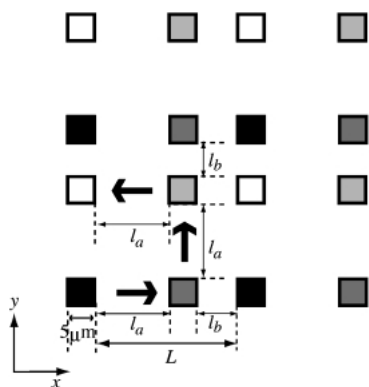


Fig. 1. Final patterns obtained as follows: (1) black squares, which are original mask patterns and are arranged at the various distances $L = 17\text{--}23\ \mu\text{m}$ are irradiated, (2) the mask is moved along the arrow to dark-grey ones and they are irradiated, (3) light-grey ones, and (4) white ones. Finally, square patterns of $L = l_a + l_b + 5$ are obtained in the film.

cal K.K.) was added as a photoinitiator. After stirring for 24 h, the sol was filtered with a $0.2\text{-}\mu\text{m}$ -pore-size membrane and dip-coated on glass substrates. The resultant gel films were prebaked for 20 min at 110°C and irradiated with UV light through a mask with $5\ \mu\text{m} \times 5\ \mu\text{m}$ square apertures. A Xe lamp (LS-140UV, Sumita Optical Glass Inc.) of $7\ \text{mW}/\text{cm}^2$ power was used for UV irradiation. **Figure 1** shows the final patterns obtained as follows: (1) black squares, which were apertures in the original mask and were arranged at various distances $L = 17\text{--}23\ \mu\text{m}$, were irradiated with UV for 2 min; (2) the mask was moved l_a (μm) in the x -axis, and dark-grey squares were irradiated for 2 min; (3) the mask was moved to l_a (μm) in the y -axis and light-grey squares were irradiated for 2 min; (4) the mask moved $-l_a$ (μm) in the x -axis and white squares were irradiated for 2 min. Finally, square patterns arranged at two distances, i.e., l_a and l_b (μm) ($l_b = L - l_a - 5$), between neighboring squares were obtained in the film. The irradiated film was developed in 1-PrOH, and the unirradiated portion was removed. The remaining patterns were postbaked at 150°C for 30 min.

After postbaking, film thickness was measured by a surface profiler. The remaining structures were imaged by scanning electron microscopy (SEM; JSM-5310, JEOL). In situ observation during the drying was carried out by optical microscopy in order to investigate top-gathering phenomena.

3. Results

Thick gel films were prepared by dip-coating. Films of 3.0 to $7.5\ \mu\text{m}$ thickness were obtained by controlling drawing speed. For preparing thick films of 14 to $23\ \mu\text{m}$ thickness, the dip-coating was repeated twice. Films of $16\ \mu\text{m}$ thickness were used in the procedures below.

Figure 2 shows SEM images of 2D arrays for $l_a = l_b$. In Figs. 2(a) and (b), 2D arrays were fabricated through the mask, which was moved (a) $l_a = l_b = 9\ \mu\text{m}$ and (b) $l_a = l_b = 7\ \mu\text{m}$, respectively. In Fig. 2(a), pillars remain vertical to the glass substrate. The corners of each pillar were removed and the shapes of the pillars differed from those of the mask patterns, as shown in Fig. 1, because photopolymerization was not sufficient and the irradiated patterns partially dissolved in the developer. In the case of $l_a = l_b = 8\ \mu\text{m}$ (which was not shown in the figures), the pillars remain vertical to the substrate as in the case of $l_a = l_b = 9\ \mu\text{m}$. In Fig. 2(b) ($l_a = l_b =$

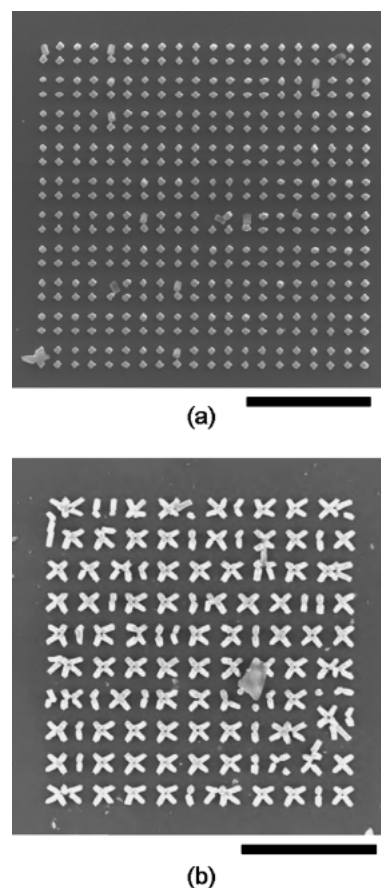


Fig. 2. SEM images of pillar arrays fabricated for (a) $l_a = l_b = 9\ \mu\text{m}$ and (b) $l_a = l_b = 7\ \mu\text{m}$. The bar is $100\ \mu\text{m}$.

$7\ \mu\text{m}$), top-gathering pillars formed. Several pillars gathered at the top and top-gathering units formed. Generally, pillars gathered in fours, but they also gathered in twos, threes, and sixes. When l_a and l_b are smaller than $7\ \mu\text{m}$ ($l_a = l_b < 7\ \mu\text{m}$), top-gathering units were also obtained as in the case of $l_a = l_b = 7\ \mu\text{m}$. From the SEM images, the critical l_a and l_b , in which pillars cannot remain vertical to substrate and top-gathering units are obtained, are $7\ \mu\text{m}$.

Figure 3 shows SEM images of other pillar arrays, which were fabricated by four irradiations at $l_a \neq l_b$: (a) $l_a = 7\ \mu\text{m}$, $l_b = 5\ \mu\text{m}$ ($l_a > l_b$) and (b) $l_a = 7\ \mu\text{m}$, $l_b = 9\ \mu\text{m}$ ($l_a < l_b$). Figs. 3(a-2) and (b-2) are enlarged images of Figs. 3(a-1) and (b-1), respectively.

In Figs. 3(a-1) and (a-2), top-gathering pillars were observed, and two or four pillars gathered at the top. The distance between the pillars that gathered is $5\ \mu\text{m}$ as shown in Fig. 3(a-2). In the 2D array, except for the edge of the array, most pillars gather in fours and form gathering units, and top-gathering units are arranged periodically. In the edge of the array, most top-gathering units are formed by two pillars. Similar structures can be obtained when l_a is larger than l_b and l_b is smaller than $8\ \mu\text{m}$. In Figs. 3(b-1) and (b-2), when l_a is smaller than l_b , most pillars gathered in fours at the top, and the distance between neighboring top-gathering pillars is $7\ \mu\text{m}$. These top-gathering units arrange periodically and top-gathering periodic arrays are obtained.

It was found from the SEM images obtained that top-gathering pillars can be formed when the distance between pillars is shorter than $8\ \mu\text{m}$ regardless of whether $l_a = l_b$ or

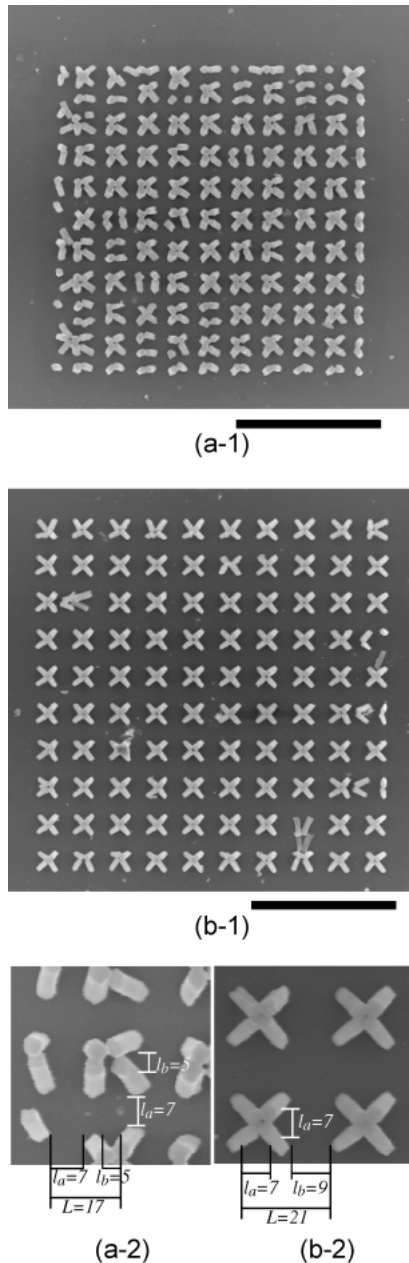


Fig. 3. SEM images of pillar arrays fabricated for (a) $l_a=7$, $l_b=5$ μm and (b) $l_a=7$, $l_b=9$ μm . The bar is 100 μm . (a-2) and (b-2) are enlarged images of (a-1) and (b-1), respectively.

$l_a \neq l_b$, and top-gathering periodic arrays can be fabricated for $l_a \neq l_b$.

To investigate the drying, we carried out the in situ observation of pillars during the drying by optical microscopy. **Figure 4** shows continuous image shots of the 2D pillar arrays every 1 s from the start of drying. In Figs. 4(a) and (b), pillar arrays formed when the distances between the pillars were $l_a = l_b = 9$ μm and $l_a = 4$ μm , $l_b = 10$ μm , respectively.

In Fig. 4(a), at the first stage, 1-PrOH dries from around the 2D arrays. At the second stage, the pillars formed seemingly approach each other, as shown in 1–3-s images. At the third stage (3-s image), the drying proceeds from the edge of the 2D array to the center. At the fourth stage (4-s image), 1-PrOH dries in the surrounding area of the pillar array but remains partially in the central area. The drying of wet 2D arrays is not

homogeneous. Then, at the final stage, all the solvent is evaporated. After the drying, pillars return to their original positions, and most of them remain vertical to the substrate.

In Fig. 4(b), firstly, 1-PrOH also dries from the edge of the 2D array. Secondly, neighboring pillars similarly approach each other forming groups of four in 3–4-s images. Finally, pillars fail to return to their original positions and remain stuck to each other in 5–7-s images.

4. Discussion

Top-gathering phenomena are observed in the drying. Therefore, the capillary force induced by the surface tension of the developer between neighboring pillars is the most plausible cause of “top-gathering.” **Figure 5** shows a cross-sectional model of pillar arrays separated by l_x and immersed in the developer. The developer dries from the edge of the 2D array to the central part (see Fig. 4, in the in situ observation). When the developer evaporates from the edge, the pillars experience a capillary force (indicated by arrows) that works toward the inside of the pillar array as shown in Fig. 5 (a). By this capillary force, two pillars approach each other and bend δ as shown in Fig. 5(b).

Two pillars immersed in liquid generate the force P , known as capillary force,¹⁴⁾

$$P = \frac{2\pi d_y h \sigma \cos \theta}{l_x} \quad (1)$$

where σ is the surface tension, θ is the contact angle of the developer, and d_y and h are the depth and height of the pillars. On the other hand, bending pillars, which tend to return to their original position, show the restoring power F expressed as⁴⁾

$$F = \frac{2d_x d_y^3}{3h^4} E \delta \quad (2)$$

where d_x is the width of the pillars, E is Young’s modulus of the pillars and δ is the sway values (see Fig. 5(b)).

In this case, the width d_x , depth d_y and height h of the pillars are 5 μm , 5 μm and 16 μm , respectively. When the distance between neighboring pillars is greater than 7 μm , F is larger than P , and the pillars return to their original position, as shown in Figs. 2(a) ($l_a = l_b = 9$ μm) and 4(a) ($l_a = l_b = 9$ μm , in-situ observation). P increases with decreasing distance between neighboring pillars. Thus, when the distance is smaller than 8 μm , as shown in Fig. 2(b) ($l_a = l_b = 7$ μm), neighboring pillars come closer easily and they stick to each other by a strong capillary force: this phenomena is top-gathering.

For $l_a = l_b$, however, drying speed in actual cases is not uniform everywhere (for example, see in Fig. 4(a)). Thus, the capillary force does not work periodically in the 2D array. As shown in Fig. 2(b), different drying speeds in the 2D array make it difficult to control arrangement of top-gathering units.

When the distance between pillars differs ($l_a \neq l_b$), the capillary force between closely spaced pillars is larger than that between widely separated pillars. Due to the imbalance in the distances between neighboring pillars, i.e., l_a and l_b , the capillary force works effectively between pillars of short distances, resulting in top-gathering units of four pillars and periodic array of top-gathering units.

We also found an important relation between l_a and l_b for the formation of periodic array of top-gathering units. For $l_a > l_b$ ($l_a = 7$ $\mu\text{m} > l_b = 5$ μm in Fig. 3(a)), the capillary force between nearest-neighbor pillars is smaller than that between

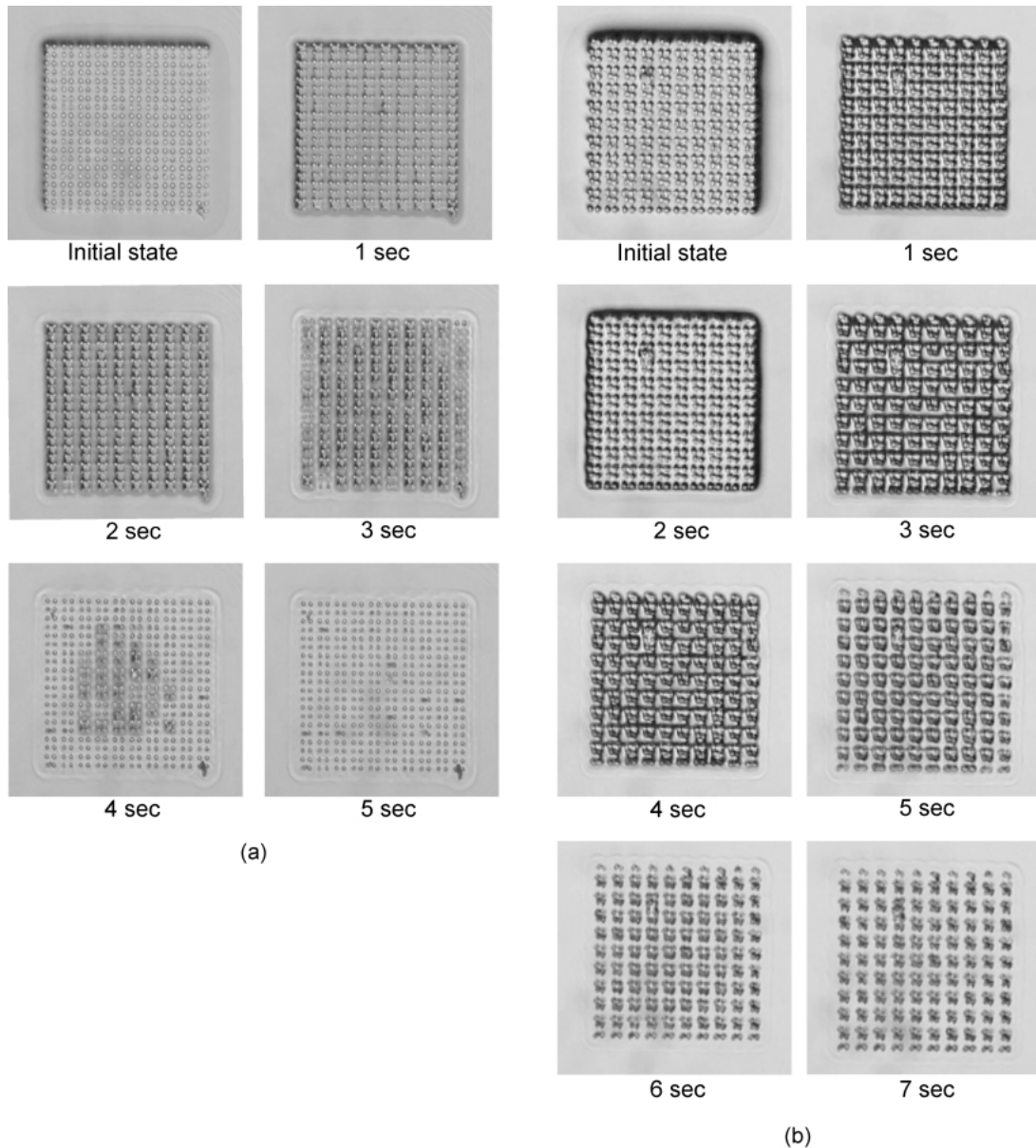


Fig. 4. Continuous image shots of drying of 2D pillar arrays: (a) $l_a = l_b = 9 \mu\text{m}$ and (b) $l_a = 4, l_b = 10 \mu\text{m}$.

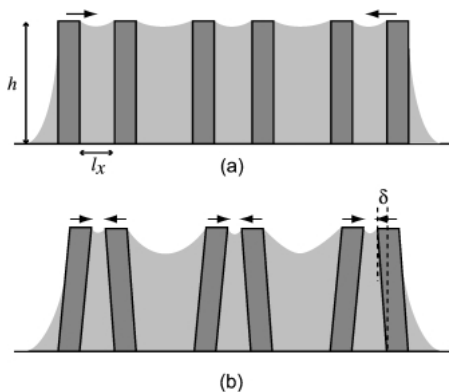


Fig. 5. Cross-sectional model of pillar arrays during drying.

second-nearest-neighbor ones. Thus, at the edge of the 2D array, top-gathering units of two pillars each were observed.

For $l_a < l_b$ ($l_a = 7 \mu\text{m} < l_b = 9 \mu\text{m}$ in Fig. 3 (b)), however, at the edge of the array, top-gathering units of four pillars each were formed easily, and uniform periodic patterns were obtained.

From SEM images of the resultant 2D array patterns and the in situ observation of the drying, we clarify following factors for the top-gathering: (1) the balance of capillary force and restoring power determines the start of top-gathering, (2) the distance between neighboring pillars ($< 8 \mu\text{m}$) is a key factor for determining capillary force, and (3) uniform patterns of four top-gathering pillars are obtained when $l_a \neq l_b$.

5. Conclusions

In summary, we produced hybrid organic-inorganic pillar arrays by the photolithography through a mask. Top-gathering pillar arrays of $16 \mu\text{m}$ height could be obtained when the distance of neighboring pillars is smaller than $8 \mu\text{m}$. It was found that top-gathering is caused by the balance of capillary force and restoring power. When the distance between neighboring pillars differs, closely spaced pillars gather and

stick to each other by a strong capillary force. By several times irradiations, capillary force was controlled periodically and gathering units of four pillars each were arranged, resulting in top-gathering periodic arrays that can be applied in new optical devices.

References

- 1) Joannopoulos, J. D., Meade, R. D. and Winn, J. N., "Photonic Crystals," Princeton University Press (1995) pp. 54-77.
- 2) Krauss, T., Song, Y. P., Thoms, S., Wilkinson, C. D. W. and DelaRue, R. M., *Electro. Lett.*, Vol. 30, pp. 1444-1446 (1994).
- 3) Herzig H. P., ed., "Micro-optics," Taylor & Francis, London (1997) pp. 87-126.
- 4) Tanaka, T., Norigami, M. and Atoda, N., *Jpn. J. Appl. Phys.*, Vol. 32, pp. 6059-6064 (1993).
- 5) Deguchi, K., Miyoshi, K., Ishi, T. and Matsuda, T., *Jpn. J. Appl. Phys.*, Vol. 31, pp. 2954-2958 (1992).
- 6) Yamabe, M., *J. Microlitho. Microfab. Microsyst.*, Vol. 4, 011005 (2005).
- 7) Geim, A. K., Dubonos, S. V., Grigorieva, I. V., Novoselov, K. S., Zhukov, A. A. and Yu. Sapoval, S., *Nature Mater.*, Vol. 2, pp. 461-463 (2003).
- 8) Segawa, H., Yamaguchi, S., Yamazaki, Y., Yano, T. and Shibata, S., *Appl. Phys. A*, to be submitted.
- 9) Kondo, T., Matsuo, S., Juodkakis, A. and Misawa, H., *Appl. Phys. Lett.*, Vol. 79, pp. 725-727 (2001).
- 10) Segawa, H., Misawa, H. and Matsuo, S., *Appl. Phys. A*, Vol. 79, pp. 407-409 (2004).
- 11) Segawa, H., Yoshida, K., Kondo, T., Matsuo, S. and Misawa, H., *J. Sol-Gel Sci. Tech.*, Vol. 26, pp. 1023-1027 (2003).
- 12) Tohge, N., Zhao, G. and Chiba, F., *Thin Solid Films*, Vol. 351, pp. 85-90 (1999).
- 13) Saifullah, M. S. M., Namatsu, H., Yamaguchi, T., Yamazaki, K. and Kurihara, K., *Jpn. J. Appl. Phys.*, Vol. 38, pp. 7052-7058 (1999).
- 14) Israelachvili, J. N., "Intermolecular and Surface Forces," 2nd ed., Academic Press, London (1992) pp. 330-333.